《原子核物理评论》
www.npr.ac.cn Nuclear Physics Review
Started in 1984

非对称夸克物质中的声速

解重龙　贺伟博　李志鹏　邵国运

Speed of Sound in Asymmetric Quark Matter

XIE Chonglong, HE Weibo, LI Zhipeng, SHAO Guoyun

在线阅读 View online: https://doi.org/10.11804/NuclPhysRev.41.2023CNPC29

引用格式:
解重龙，贺伟博，李志鹏，邵国运．非对称夸克物质中的声速[J]．原子核物理评论，2024，41(1):587-593．doi: 10.11804/NuclPhysRev.41.2023CNPC29
XIE Chonglong, HE Weibo, LI Zhipeng, SHAO Guoyun. Speed of Sound in Asymmetric Quark Matter[J]. Nuclear Physics Review, 2024, 41(1):587-593. doi: 10.11804/NuclPhysRev.41.2023CNPC29

Article ID: 1007-4627(2024)01–0587–07

Speed of Sound in Asymmetric Quark Matter

XIE Chonglong[1], HE Weibo[2], LI Zhipeng[1], SHAO Guoyun[1,†]

(*1. MOE Key Laboratory for Non-equilibrium Synthesis and Modulation of Condensed Matter, School of Physics, Xi'an Jiaotong University, Xi'an 710049, China*;
2. School of Physics, Peking University, Beijing 100871, China)

Abstract: The speed of sound in quark matter is an important physical quantity for studying the properties and the spacetime evolution of quark-gluon plasma (QGP). The behavior of the speed of sound with respect to temperature and density can reveal to some extent the equation of state and the phase structure of QGP. Building upon the previous studies on the speed of sound in symmetric quark matter, the formulae for calculating the speed of sound in asymmetric quark matter in the temperature-density space are further derived. The PNJL model is then used to calculate the dependence of the speed of sound on isospin asymmetry. Furthermore, the relationship between the magnitude of the speed of sound and the QCD phase structure is discussed, and the regions where the acoustic equation fails are indicated under different physical conditions. It is found that the boundary of vanishing sound speed in asymmetric quark matter is smaller than that in symmetric quark matter, meaning that the range where the acoustic wave equation fails in asymmetric quark matter is smaller than that in symmetric quark matter. The results also indicate that in most of the stable phase, the speed of sound in asymmetric quark matter is slightly larger than that in symmetric quark matter.

Key words: quark-gluon plasma; equation of state; speed of sound

CLC number: O571.6 **Document code:** A **DOI:** 10.11804/NuclPhysRev.41.2023CNPC29

0 Introduction

Exploring the equation of state (EOS) and the phase structure of quark gluon plasma (QGP) is a hot topic in nuclear physics[1−15]. The speed of sound in QGP is a crucial mechanical characteristic to describe the variation of EOS. Its dependence on temperature and baryon density carries important information in describing the evolution of a fireball and the final observables. Recently, there have been some attempts to extract the speed of sound of QGP from the experimental data. For example, the studies indicate that the speed of sound is a function of charged particle multiplicity $\langle \mathrm{d}N_{\mathrm{ch}}/\mathrm{d}\eta \rangle$ [16−17]. An interesting method to estimate the speed of sound is proposed by building its connection with the net baryon number cumulants and the quantum chromodynamics (QCD) phase structure[18].

Besides, there has been growing interest in the speed of sound in neutron star matter[19−21]. The variation of the speed of sound with baryon density affects the mass-radius relation and the tidal deformability of neutron stars, and provides a useful probe for studying the EOS of neutron star matter. To obtain a neutron star with a mass greater than twice that of the sun, some studies show that the EOS of neutron star matter must be sufficiently stiff in some density range, corresponding to a speed of sound squared much greater than 1/3[22−28]. The speed of sound in neutron star matter is also connected to the gravitational wave frequencies induced by the g-mode oscillation of a neutron star[29]. Furthermore, the magnitude of speed of sound affects the dynamics of primordial density perturbations in the era of cosmic QCD phase transition, which is relevant for the induced gravitational wave signals[30].

Some calculations about the speed of sound in QCD matter have been performed in lattice QCD[31−35], (P)NJL model[36−40], quark-meson coupling model[7, 41], hadron resonance gas (HRG) model[42−43], field correlator method (FCM)[44−45] and quasiparticle model[46]. In particular, the relationship between the speed of sound and the QCD phase transition has been intensively studied[47−48]. The numerical results indicate that the dependence of the speed of sound on the system parameters (temperature, density and chemical potential) is closely related to the phase structure

Received date: 30 Jun. 2023; **Revised date:** 30 Jan. 2024

Foundation item: National Natural Science Foundation of China (11875213); Natural Science Basic Research Plan in Shaanxi Province of China (2024JC-YBMS-018)

Biography: XIE Chonglong(2000−), mail, Huanggang, Hubei Province, graduate student, working on nuclear physics

† **Corresponding author:** SHAO Guoyun, E-mail: gyshao@xjtu.edu.cn

of QCD.

By far, the studies in the literature mainly focus on the speed of sound in symmetric quark matter, and there is a lack of systematic research on the speed of sound in the isospin asymmetric quark matter. In this work we will explore the behavior of the speed of sound in asymmetric quark matter. On the one hand, we will derive the formulae for calculating the speed of sound in asymmetric quark matter with two conserved charges. On the other hand, we will demonstrate numerically the dependence of the speed of sound on isospin asymmetric parameter in the PNJL model. The relevant research has certain significance in exploring the equation of state of QCD and the evolution of QGP.

1 Formula of speed of sound in asymmetric quark matter and the PNJL quark model

The general definition of speed of sound is

$$c_X^2=\left(\frac{\partial p}{\partial \epsilon}\right)_X, \tag{1}$$

where p and ϵ are pressure and energy density. A specifying constant quantity X is required to describe the propagation of the compression wave through a medium. For a fireball created in relativistic heavy-ion collisions, it evolves with a constant entropy density to baryon number density ratio $s/\rho_{\rm B}$ under the ideal fluid approximation. Therefore, the speed of sound can be calculated along the isentropic curve

$$c_{s/\rho_{\rm B}}^2=\left(\frac{\partial p}{\partial \epsilon}\right)_{s/\rho_{\rm B}}. \tag{2}$$

In practice the above definition can only be used to calculate the speed of sound along isentropic trajectories. To calculate the speed of sound throughout the full phase diagram, it is necessary to derive the corresponding formula as a function of temperature T and baryon number density $\rho_{\rm B}$. With the fundamental thermodynamic relation, Eq. (2) can be rewritten as

$$\begin{aligned}c_\sigma^2=\left(\frac{\partial p}{\partial \epsilon}\right)_\sigma=\frac{\partial(p,\sigma)}{\partial(\epsilon,\sigma)}=\frac{\partial(p,\sigma)}{\partial(T,\rho_{\rm B})}\Big/\frac{\partial(\epsilon,\sigma)}{\partial(T,\rho_{\rm B})}=\\ \begin{vmatrix}\left(\frac{\partial p}{\partial T}\right)_{\rho_{\rm B}} & \left(\frac{\partial p}{\partial \rho_{\rm B}}\right)_T\\ \left(\frac{\partial \sigma}{\partial T}\right)_{\rho_{\rm B}} & \left(\frac{\partial \sigma}{\partial \rho_{\rm B}}\right)_T\end{vmatrix}\Bigg/\begin{vmatrix}\left(\frac{\partial \epsilon}{\partial T}\right)_{\rho_{\rm B}} & \left(\frac{\partial \epsilon}{\partial \rho_{\rm B}}\right)_T\\ \left(\frac{\partial \sigma}{\partial T}\right)_{\rho_{\rm B}} & \left(\frac{\partial \sigma}{\partial \rho_{\rm B}}\right)_T\end{vmatrix}=\\ \frac{\left(\frac{\partial p}{\partial T}\right)_{\rho_{\rm B}}\left(\frac{\partial \sigma}{\partial \rho_{\rm B}}\right)_T-\left(\frac{\partial p}{\partial \rho_{\rm B}}\right)_T\left(\frac{\partial \sigma}{\partial T}\right)_{\rho_{\rm B}}}{\left(\frac{\partial \epsilon}{\partial T}\right)_{\rho_{\rm B}}\left(\frac{\partial \sigma}{\partial \rho_{\rm B}}\right)_T-\left(\frac{\partial \epsilon}{\partial \rho_{\rm B}}\right)_T\left(\frac{\partial \sigma}{\partial T}\right)_{\rho_{\rm B}}},\end{aligned} \tag{3}$$

where $\sigma=s/\rho_{\rm B}$ is defined for convenience.

The speed of sound will be calculated under the physical condition that the number density of strange quark is zero $\rho_{\rm s}=0$, which is the requirement of strangeness conservation in strong interaction. The asymmetric parameter α is defined as the ratio of u, d quark number density $\alpha=\rho_{\rm u}/\rho_{\rm d}$. Then, we can derive the following formulae in the grand canonical ensemble

$$\mathrm{d}p=s\mathrm{d}T+\sum_{i=\mathrm{u,d,s}}\rho_i\mathrm{d}\mu_i=s\mathrm{d}T+\frac{3}{\alpha+1}\rho_{\rm B}(\alpha\mathrm{d}\mu_{\rm u}+\mathrm{d}\mu_{\rm d}), \tag{4}$$

$$\left(\frac{\partial p}{\partial T}\right)_{\rho_{\rm B}}=s+\frac{3}{\alpha+1}\rho_{\rm B}\left[\alpha\left(\frac{\partial \mu_{\rm u}}{\partial T}\right)_{\rho_{\rm B}}+\left(\frac{\partial \mu_{\rm d}}{\partial T}\right)_{\rho_{\rm B}}\right], \tag{5}$$

$$\left(\frac{\partial p}{\partial \rho_{\rm B}}\right)_T=\frac{3}{\alpha+1}\rho_{\rm B}\left[\alpha\left(\frac{\partial \mu_{\rm u}}{\partial \rho_{\rm B}}\right)_T+\left(\frac{\partial \mu_{\rm d}}{\partial \rho_{\rm B}}\right)_T\right], \tag{6}$$

$$\mathrm{d}\epsilon=T\mathrm{d}s+\sum_{i=\mathrm{u,d,s}}\mu_i\mathrm{d}\rho_i=T\mathrm{d}s+\frac{3}{\alpha+1}(\alpha\mu_{\rm u}+\mu_{\rm d})\mathrm{d}\rho_{\rm B}, \tag{7}$$

$$\left(\frac{\partial \epsilon}{\partial T}\right)_{\rho_{\rm B}}=T\left(\frac{\partial s}{\partial T}\right)_{\rho_{\rm B}}, \tag{8}$$

$$\left(\frac{\partial \epsilon}{\partial \rho_{\rm B}}\right)_T=T\left(\frac{\partial s}{\partial \rho_{\rm B}}\right)_T+\frac{3}{\alpha+1}(\alpha\mu_{\rm u}+\mu_{\rm d}), \tag{9}$$

$$\left(\frac{\partial \sigma}{\partial T}\right)_{\rho_{\rm B}}=\frac{1}{\rho_{\rm B}}\left(\frac{\partial s}{\partial T}\right)_{\rho_{\rm B}}, \tag{10}$$

$$\left(\frac{\partial \sigma}{\partial \rho_{\rm B}}\right)_T=\frac{1}{\rho_{\rm B}}\left(\frac{\partial s}{\partial \rho_{\rm B}}\right)_T-\frac{s}{\rho_{\rm B}^2}. \tag{11}$$

In the above formulae, $\mu_{\rm u}$, $\mu_{\rm d}$ represent the chemical potential of u, d quark. For a given asymmetric parameter α, Eq. (3) can be used to calculate the speed of sound in the $T-\rho_{\rm B}$ plane with these formulae. For the case of $\alpha=1$, these formulae return to those for symmetric quark matter.

In the numerical calculation, we take the 2+1 flavor PNJL quark model. the Lagrangian density is written as

$$\begin{aligned}\mathcal{L}=&\bar{q}(\mathrm{i}\gamma^\mu D_\mu+\gamma_0\hat{\mu}-\hat{m}_0)q+G\sum_{k=0}^{8}[(\bar{q}\lambda_k q)^2+(\bar{q}\mathrm{i}\gamma_5\lambda_k q)^2]-\\ &K[\det{}_f(\bar{q}(1+\gamma_5)q)+\det{}_f(\bar{q}(1-\gamma_5)q)]-\\ &U(\Phi[A],\bar{\Phi}[A],T),\end{aligned} \tag{12}$$

where q denotes the quark fields with three flavors, u, d, and s; $\hat{m}_0=\mathrm{diag}(m_{\rm u}, m_{\rm d}, m_{\rm s})$ in flavor space; G and K are the four-point and six-point interacting constants, respectively. The $\hat{\mu}=\mathrm{diag}(\mu_{\rm u}, \mu_{\rm d}, \mu_{\rm s})$ are the quark chemical potentials. The covariant derivative in the Lagrangian is defined as $D_\mu=\partial_\mu-\mathrm{i}A_\mu$. The gluon background field $A_\mu=\delta_\mu^0 A_0$ is supposed to be homogeneous and static, with

$A_0 = g\mathcal{A}_0^\alpha \frac{\lambda^\alpha}{2}$, where $\frac{\lambda^\alpha}{2}$ is the SU(3) color generators. The effective potential $U(\Phi[A], \bar{\Phi}[A], T)$ is expressed with the traced Polyakov loop $\Phi = (\mathrm{Tr}_c L)/N_C$ and its conjugate $\bar{\Phi} = (\mathrm{Tr}_c L^\dagger)/N_C$. The Polyakov loop L is a matrix in color space

$$L(\boldsymbol{x}) = \mathcal{P}\exp\left[\mathrm{i}\int_0^\beta \mathrm{d}\tau A_4(\boldsymbol{x},\tau)\right], \tag{13}$$

where $\beta = 1/T$ is the inverse of temperature and $A_4 = \mathrm{i}A_0$.

The Polyakov-loop effective potential is

$$\frac{U\left(\Phi,\bar{\Phi},T\right)}{T^4} = -\frac{a(T)}{2}\bar{\Phi}\Phi + b(T)\ln\left[1-6\bar{\Phi}\Phi + 4(\bar{\Phi}^3+\Phi^3) - 3(\bar{\Phi}\Phi)^2\right], \tag{14}$$

where

$$a(T) = a_0 + a_1\left(\frac{T_0}{T}\right) + a_2\left(\frac{T_0}{T}\right)^2 \text{ and } b(T) = b_3\left(\frac{T_0}{T}\right)^3. \tag{15}$$

The parameters $a_0 = 3.51$, $a_1 = -2.47$, $a_2 = 15.2$, $b_3 = -1.75$ and $T_0 = 270$ MeV are fitted according to the earlier lattice simulation of QCD thermodynamics in the pure gauge sector[49]. When the quark fields are included $T_0 = 210$ MeV will be implemented to describe well the thermodynamics and phase transition of QCD. The constituent quark mass in the mean field approximation can be derived as

$$M_i = m_i - 4G\phi_i + 2K\phi_j\phi_k \qquad (i \neq j \neq k), \tag{16}$$

where ϕ_i stands for quark condensate of the flavor i.

The thermodynamic potential of bulk quark matter is derived as

$$\begin{aligned}\Omega =& U(\bar{\Phi},\Phi,T) + 2G\left(\phi_\mathrm{u}^2+\phi_\mathrm{d}^2+\phi_\mathrm{s}^2\right) - 4K\phi_\mathrm{u}\phi_\mathrm{d}\phi_\mathrm{s} - \\ & 2\int_\Lambda \frac{\mathrm{d}^3p}{(2\pi)^3}3(E_\mathrm{u}+E_\mathrm{d}+E_\mathrm{s}) - \\ & 2T\sum_{i=\mathrm{u,d,s}}\int\frac{\mathrm{d}^3p}{(2\pi)^3}(Q_1+Q_2),\end{aligned} \tag{17}$$

where $Q_1 = \ln(1+3\Phi\mathrm{e}^{-(E_i-\mu_i)/T} + 3\bar{\Phi}\mathrm{e}^{-2(E_i-\mu_i)/T} + \mathrm{e}^{-3(E_i-\mu_i)/T})$, $Q_2 = \ln(1+3\bar{\Phi}\mathrm{e}^{-(E_i+\mu_i)/T} + 3\Phi\mathrm{e}^{-2(E_i+\mu_i)/T} + \mathrm{e}^{-3(E_i+\mu_i)/T})$, and $E_i = \sqrt{\boldsymbol{p}^2+M_i^2}$ is the dispersion relation. The pressure and energy density can be derived using the thermodynamic relations in the grand canonical ensemble as

$$p = -\Omega, \quad \epsilon = -p + Ts + \sum_{i=\mathrm{u,d,s}}\mu_i\rho_i. \tag{18}$$

For the given temperature T, baryon density ρ_B and asymmetric parameter α, the values of ϕ_u, ϕ_d, ϕ_s, Φ, $\bar{\Phi}$, μ_u, μ_d and μ_s can be determined by solving the equations derived by minimizing the thermodynamic potential

$$\frac{\partial\Omega}{\partial\phi_\mathrm{u}} = \frac{\partial\Omega}{\partial\phi_\mathrm{d}} = \frac{\partial\Omega}{\partial\phi_\mathrm{s}} = \frac{\partial\Omega}{\partial\Phi} = \frac{\partial\Omega}{\partial\bar{\Phi}} = 0. \tag{19}$$

In the numerical calculation, a cut-off Λ is implemented in the three-momentum space for divergent integrations. The model parameters are taken with: $\Lambda = 602.3$ MeV, $G\Lambda^2 = 1.835$, $K\Lambda^5 = 12.36$, $m_{\mathrm{u,d}} = 5.5$ and $m_\mathrm{s} = 140.7$ MeV, determined by fitting $f_\pi = 92.4$ MeV, $M_\pi = 135.0$ MeV, $m_\mathrm{K} = 497.7$ MeV and $m_\eta = 957.8$ MeV[50].

2 Numerical results and discussions

We first present in Fig. 1 the isentropic curves for $\sigma = 50, 10, 5, 1$ in the T-μ_B plane. Each curve in this figure corresponds to an evolutionary trajectory of QGP generated with a specific collision energy. For the two cases of $\sigma = 50$ and 10, the fireball only passes through the stable phase during the evolution. However for the cases of $\sigma = 5$ and 1, both the metastable and unstable phases are involved. The behaviors of σ in the T-μ_B plane is mainly determined by the phase structure of the system. In theory, for a fermion system with the temperature and density dependent dynamic mass, there usually exists a first-order phase transition at low temperature. Numerical calculations in different systems show that the qualitative behaviors of s/ρ_B are similar to the curves shown in Fig. 1. For the liquid-gas phase transition in nuclear matter, we also derived the similar curves of s/ρ_B[48]. Generally, the appearance of the inflection point does not directly corresponds to the position of the phase transition, but the crossover phase transition of QCD at high temperature can induce some perturbation on s/ρ_B, as shown in the curve of $\sigma = 50$.

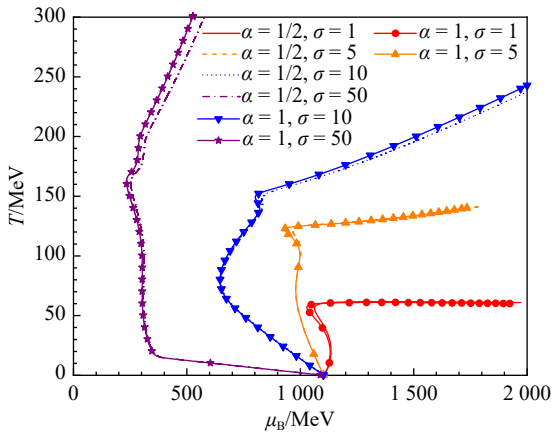

Fig. 1　Isentropic curves for $\sigma = 50, 10, 5, 1$ for both the symmetric and asymmetric quark matter in the T-μ_B plane. (color online)

We plot in Fig. 2 the EOSs of quark matter along different evolutionary paths given in Fig. 1. The numerical results show that for the cases of $\sigma = 1$ and 5 in symmetric matter and $\sigma = 1$ in asymmetric matter, the pressure of the system has a maximum and a minimum as the energy density increases, respectively. The region between the maximum and minimum approximately correspond to (lies in exactly) the unstable phase of the system. After passing

through the minimum, the pressure grows rapidly with the increase of energy density. For the cases of $\sigma = 5$ in asymmetric quark matter and $\sigma = 10$ and 50 in both the symmetric and asymmetric quark matter, the pressure increases monotonically with the rising energy density. Figure 2 also indicates that the equations of state of asymmetric matter are stiffer than those of symmetric matter, although it is not obvious for the case of $\sigma = 50$. These behaviors of the equations of state under different physical conditions determine the speed of sound in quark matter.

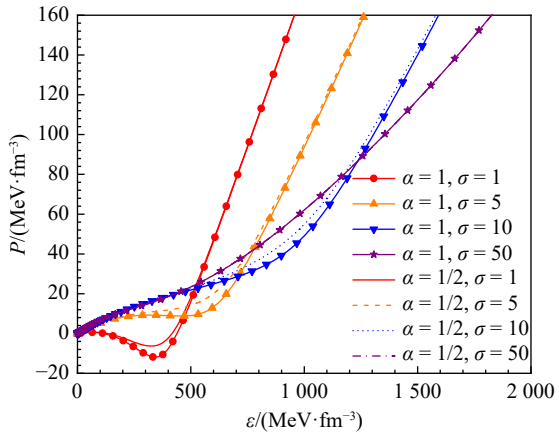

Fig. 2 EOSs along the different evolutionary paths shown in Fig. 1. (color online)

The evolving behaviors of the speed of sound corresponding to the EOSs under different conditions in Fig. 2 are plotted in Fig. 3. This figure demonstrates that the influence of isospin effect on the speed of sound of quark matter. In the chiral restored phase (the high-temperature and/or high-density region), the isospin splitting effect is relatively smaller, because the differences of both the quark masses and chemical potentials between u and d quarks are very small, leading to that the asymmetric parameter α has a weak effect on the EOSs. The isospin effect is also weak at lower density (lower energy density) in the chiral broken phase with the similar reasons for the chiral restored phase, in particular when the mass of u quark is the same as that of d quark. However, the isospin effect has a relatively larger influence on the EOSs at intermediate density and in the phase transition region. Therefore, from the low-temperature and low-density region to the high-temperature and/or high-density region, the influence of the isospin effect on EOSs goes from weak to strong and then to weak again, which is consistent with the results shown in Fig. 2. With the combination of the above qualitative analysis and the EOSs in Fig. 2, as well as the isetropic trajectories in Figs. 1, 4 and 5, it can be understood that when σ is relatively smaller (*e.g.*, $\sigma = 1$, 5, 10), the speed of sound of asymmetric quark is larger than that of symmetric quark matter in the phase transition region, and a reversal happens when approaching the chiral restored phase. while for $\sigma = 50$, the sound speed curves of the symmetric and asymmetric quark mater almost coincide because the isentropic curves of them mainly pass through the low-density region and the chiral restored phase at high temperature.

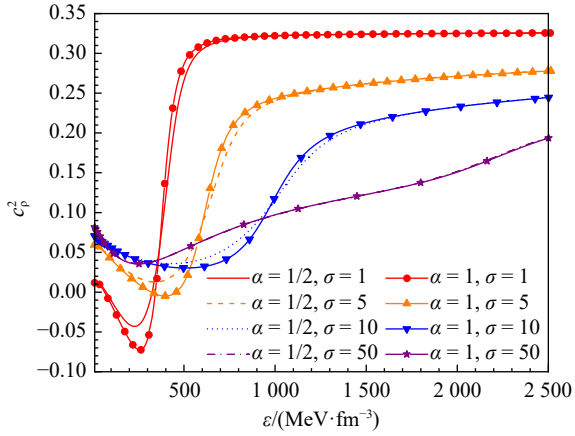

Fig. 3 Square of speed of sound for the EOSs under different conditions along the evolutionary paths shown in Fig. 1. (color online)

To demonstrate the dependence of the speed of sound on temperature and density, we present the contour plots of the speed of sound in both the symmetric quark matter and asymmetric quark matter in Figs. 4 and 5, respectively. From the two figures, it can be seen that in the low-temperature region of the first-order phase transition, the restoration of chiral symmetry causes the square of the speed of sound to quickly approach 1/3, as indicated by the red curve in Fig. 3. In the smooth transition region at high temperatures, the growth of the speed of sound with increasing temperature or density is relatively slower. However, at extremely high temperatures and densities, the square of the speed of sound still approaches 1/3.

The red solid lines in Figs. 4 and 5 correspond to the boundaries where the speed of sound becomes zero with the condition of $\left(\frac{\partial p}{\partial \epsilon}\right)_\sigma = 0$. As pointed out in our previous study[47], the acoustic wave equation becomes a decaying

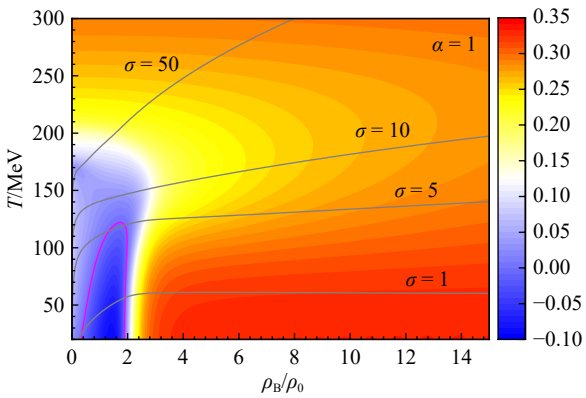

Fig. 4 Contour map of c_σ^2 in the T-ρ_B plane for symmetric quark matter with $\alpha = 1$. The red curve is the boundary of vanishing sound speed. (color online)

function within the region enclosed by the red solid lines, and the disturbances cannot propagate outwards within this region. Comparing Figs. 4 and 5, we observe that the region with the negative speed of sound squared in asymmetric matter is smaller than that in symmetric matter, which can also be seen from Fig. 3.

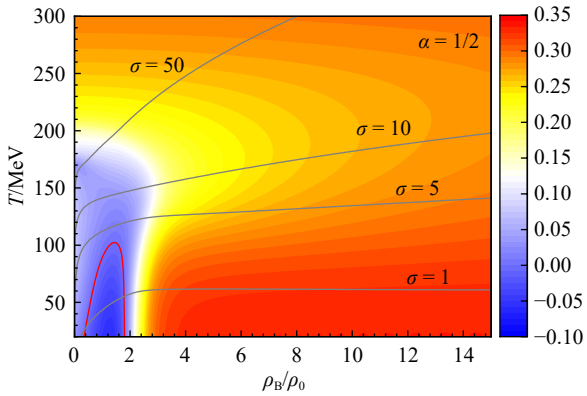

Fig. 5 Contour map of c_σ^2 in the T-ρ_B plane for asymmetric quark matter with $\alpha = 1/2$. The red curve is the boundary of vanishing sound speed. (color online)

Furthermore, combined with the contour plots of the speed of sound under the condition $\mu_u = \mu_d = \mu_s$[47], it can be observed that the condition $\rho_s = 0$ taken in this study has a significant influence on the speed of sound in quark matter, especially in the low temperature and high density region where the chiral symmetry of u and d quarks has restored. The calculation[47] demonstrates that under the condition of $\mu_u = \mu_d = \mu_s$, the speed of sound at low temperatures rapidly increases to nearly $\sqrt{1/3}$ after the restoration of chiral symmetry of u and d quarks. However, as the density increases, the presence of strange quarks causes the equation of state to become softer, resulting in a subsequent decrease of the sound speed, which tends to be $\sqrt{1/3}$ again after the restoration of chiral symmetry of s quark at higher densities.

To compare the value of the speed of sound in symmetric and asymmetric quark matter, we plotted the contour maps of $r_s = c^2_{\sigma=1/2}/c^2_{\sigma=1}$ in Fig. 6. In the gray area, the speed of sound in asymmetric quark matter is slightly larger than that in symmetric quark matter, and $r_s = 1$ on the boundary of the gray area. In the red region, $r_s < 1$, it means that the value of the speed of sound in asymmetric quark matter is smaller than that in symmetric quark matter. It should be noted that the difference in speed of sound between the two cases in the gray area is very small ($r_s < 1.005$ in most of the gray region). The negative ratio appears in the region between the two boundaries (black solid curve and dashed curve) of the vanishing sound speed. In this region, the square of the speed of sound in asymmetric quark matter is positive, while in symmetric quark matter, the mechanical instability violates the sound wave equation with the c_σ^2 being negative. The region where the ratio takes a larger absolute value locates near the boundary of (black solid curve) of the vanishing sound speed in symmetric quark matter.

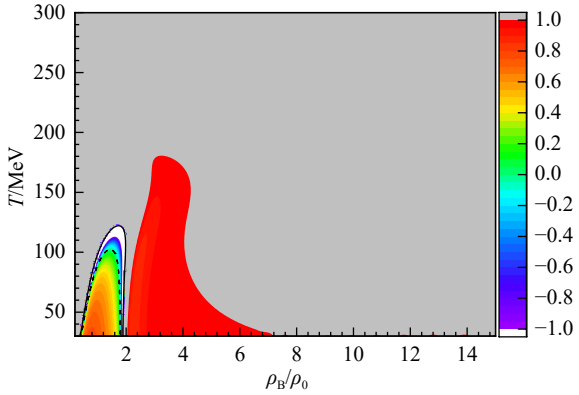

Fig. 6 Contour map of $r_s = c^2_{\sigma=1/2}/\ c^2_{\sigma=1}$ in the T-ρ_B plane. The solid (dashed) black curve is the boundary of vanishing sound speed in symmetric (asymmetric) matter. In the gray area, the squared speed of sound in asymmetric matter is slightly larger than that in the symmetric matter with $r_s > 1$; $r_s = 1$ on the boundary of the gray area; $r_s < 1$ in the red area. (color online)

3 Summary

We derived the formula for calculating the speed of sound in asymmetric quark matter in the temperature and density space, and calculated the speed of sound in the PNJL quark model. The results indicate that the boundary of vanishing sound speed in asymmetric quark matter is smaller than that in symmetric quark matter, meaning that the range where the acoustic wave equation fails in asymmetric quark matter is smaller than that in symmetric quark matter. The calculations also indicate that in most of the stable phase, the speed of sound in asymmetric quark matter is slightly larger than that in symmetric quark matter. Additionally, it should be pointed out that only the change of sound speed caused by isospin asymmetry of u, d quark chemical potential is considered in this study. The difference in u, d quark dynamic masses is not included. After introducing the isospin interactions that cause the splitting of u, d quark masses, it is expected that the isospin effects on the speed of sound will be more pronounced. The relevant research is currently underway.

Acknowledgments The work was supported by National Natural Science Foundation of China (Grant No. 11875213) and Natural Science Basic Research Plan in Shaanxi Province of China (Program No. 2024JC-YBMS-018).

References:

[1] FUKUSHIMA K. Phys Rev D, 2008, 77: 114028.

[2] RATTI C, THALER M A, WEISE W. Phys Rev D, 2006, 73: 014019.
[3] COSTA P, RUIVO M C, DE SOUSA C A, et al. Symmetry, 2010, 2(3): 1338.
[4] FU W J, ZHANG Z, LIU Y X. Phys Rev D, 2008, 77: 014006.
[5] SASAKI T, TAKAHASHI J, SAKAI Y, et al. Phys Rev D, 2012, 85: 056009.
[6] FERREIRA M, COSTA P, PROVIDÊNCIA C M C. Phys Rev D, 2014, 89: 036006.
[7] SCHAEFER B J, WAGNER M, WAMBACH J. Phys Rev D, 2010, 81: 074013.
[8] SKOKOV V, FRIMAN B, REDLICH K. Phys Rev C, 2011, 83: 054904.
[9] QIN S X, CHANG L, CHEN H, et al. Phys Rev Lett, 2011, 106: 172301.
[10] GAO F, CHEN J, LIU Y X, et al. Phys Rev D, 2016, 93: 094019.
[11] FISCHER C S, LUECKER J, WELZBACHER C A. Phys Rev D, 2014, 90: 034022.
[12] FU W J, PAWLOWSKI J M, RENNECKE F. Phys Rev D, 2020, 101: 054032.
[13] WANG X, WEI M, LI Z, et al. Phys Rev D, 2019, 99: 016018.
[14] LIU L M, XU J, PENG G X. Phys Rev D, 2021, 104: 076009.
[15] WEN X J, HE R, LIU J B. Phys Rev D, 2021, 103: 094020.
[16] GARDIM F G, GIACALONE G, LUZUM M, et al. Nature Physics, 2020, 16(6): 615.
[17] BISWAS D, DEKA K, JAISWAL A, et al. Phys Rev C, 2020, 102: 014912.
[18] SORENSEN A, OLIINYCHENKO D, KOCH V, et al. Phys Rev Lett, 2021, 127: 042303.
[19] REED B, HOROWITZ C J. Phys Rev C, 2020, 101: 045803.
[20] KANAKIS-PEGIOS A, KOLIOGIANNIS P S, MOUSTAKIDIS C C. Phys Rev C, 2020, 102: 055801.
[21] HAN S, PRAKASH M. The Astrophysical Journal, 2020, 899(2): 164.
[22] TEWS I, CARLSON J, GANDOLFI S, et al. The Astrophysical Journal, 2018, 860(2): 149.
[23] GREIF S K, RAAIJMAKERS G, HEBELER K, et al. Monthly Notices of the Royal Astronomical Society, 2019, 485(4): 5363.
[24] FORBES M M, BOSE S, REDDY S, et al. Phys Rev D, 2019, 100: 083010.
[25] DRISCHLER C, HAN S, LATTIMER J M, et al. Phys Rev C, 2021, 103: 045808.
[26] ESSICK R, TEWS I, LANDRY P, et al. Phys Rev C, 2020, 102: 055803.
[27] HAN S, MAMUN M A A, LALIT S, et al. Phys Rev D, 2019, 100: 103022.
[28] KOJO T. AAPPS Bulletin, 2021, 31(1): 11.
[29] JAIKUMAR P, SEMPOSKI A, PRAKASH M, et al. Phys Rev D, 2021, 103: 123009.
[30] ABE K T, TADA Y, UEDA I. Journal of Cosmology and Astroparticle Physics, 2021, 2021(06): 048.
[31] AOKI Y, ENDRŐDI G, FODOR Z, et al. Nature, 2006, 443(7112): 675.
[32] BORSANYI S, FODOR Z, HOELBLING C, et al. Phys Lett B, 2014, 730: 99.
[33] BAZAVOV A, BHATTACHARYA T, DETAR C, et al. Phys Rev D, 2014, 90: 094503.
[34] PHILIPSEN O. Progress in Particle and Nuclear Physics, 2013, 70: 55.
[35] BORSANYI S, FODOR Z, GUENTHER J N, et al. Phys Rev Lett, 2020, 125: 052001.
[36] MOTTA M, STIELE R, ALBERICO W M, et al. The European Physical Journal C, 2020, 80(8): 770.
[37] GHOSH S K, MUKHERJEE T K, MUSTAFA M G, et al. Phys Rev D, 2006, 73: 114007.
[38] MARTY R, BRATKOVSKAYA E, CASSING W, et al. Phys Rev C, 2013, 88: 045204.
[39] DEB P, KADAM G P, MISHRA H. Phys Rev D, 2016, 94: 094002.
[40] ZHAO Y P. Phys Rev D, 2020, 101: 096006.
[41] ABHISHEK A, MISHRA H, GHOSH S. Phys Rev D, 2018, 97: 014005.
[42] VENUGOPALAN R, PRAKASH M. Nuclear Physics A, 1992, 546(4): 718.
[43] BLUHM M, ALBA P, ALBERICO W, et al. Nuclear Physics A, 2014, 929: 157.
[44] KHAIDUKOV Z V, LUKASHOV M S, SIMONOV Y A. Phys Rev D, 2018, 98: 074031.
[45] KHAIDUKOV Z V, SIMONOV Y A. Phys Rev D, 2019, 100: 076009.
[46] MYKHAYLOVA V, SASAKI C. Phys Rev D, 2021, 103: 014007.
[47] HE W B, SHAO G Y, GAO X Y, et al. Phys Rev D, 2022, 105: 094024.
[48] HE W B, SHAO G Y, XIE C L. Phys Rev C, 2023, 107: 014903.
[49] RÖßNER S, RATTI C, WEISE W. Phys Rev D, 2007, 75: 034007.
[50] REHBERG P, KLEVANSKY S P, HÜFNER J. Phys Rev C, 1996, 53: 410.

非对称夸克物质中的声速

解重龙[1], 贺伟博[2], 李志鹏[1], 邵国运[1,†]

(1. 西安交通大学物理学院，教育部物质非平衡合成与调控重点实验室，西安 710049;
2. 北京大学物理学院，北京 100871)

摘要: 夸克物质中的声速是研究夸克-胶子等离子体(QGP)的性质和时空演化的一个重要物理量，声速随温度和密度的变化行为在一定程度上能够揭示QGP的物态方程和相结构。在之前研究对称夸克物质中声速的基础上，本工作进一步推导了在温度和密度空间计算非对称夸克物质声速的公式，并利用PNJL模型计算了夸克物质中的声速对同位旋不对称参数的依赖，讨论了声速的大小与QCD相结构的关系，指出了不同物理条件下声波方程失效的范围。结果表明，非对称夸克物质中声速平方小于零的区域小于对称夸克物质，这意味着非对称夸克物质中声波方程失效的范围小于对称夸克物质。计算还表明，在稳定相的大部分区域，非对称夸克物质中的声速略大于对称夸克物质的声速。

关键词: 夸克-胶子等离子体；状态方程；声速

收稿日期: 2023-06-30；　**修改日期:** 2024-01-30

基金项目: 国家自然科学基金资助项目(11875213), 陕西省自然科学基础研究计划(2024JC-YBMS-018)

† **通信作者:** 邵国运，E-mail: gyshao@xjtu.edu.cn